PERGAMON

International Journal of Multiphase Flow 28 (2002) 773–789

International Journal of Multiphase Flow

www.elsevier.com/locate/ijmulflow

Liquid film disintegration regimes and proposed correlations

I.S. Carvalho [a,*], M.V. Heitoyr [b], D. Santos [c]

[b] *Department of Mechanical Engineering, Instituto Superior de Engenharia de Lisboa, Rua Conselheiro Emidio Navarro 1, 1949-014 Lisbon, Portugal*

[b] *Department of Mechanical Engineering, Instituto Superior Técnico, Technical University of Lisbon, 1049-001 Lisbon, Portugal*

[c] *PROET—Projectos, Engenharia e Tecnologia S.A, Grupo EDP, 1749-061 Lisbon, Portugal*

Received 7 March 2000; received in revised form 30 November 2001

Abstract

The process of liquid sheet disintegration and break-up into a spray is studied making use of a flat liquid film surrounded by two air streams. The work considers a 2-D liquid film with an aspect ratio of 114 and a liquid velocity between 0.7 and 6.4 m/s ($543 \leqslant Re_L \leqslant 4963$) and an air velocity up to 39 m/s ($Re_G \leqslant 17\,647$), and allows to study the basic phenomena typical of airblast atomisation. The results include the quantification of instability amplitudes, break-up lengths and frequencies for the above-mentioned range of liquid (water) and air flow velocities. Three different experimental techniques are used: back light and laser light sheet illumination, to measure the instability amplitudes, which leads to the liquid film disintegration and the spray formation; strobe light illumination, for the quantification of either break-up lengths and frequencies, and; a laser attenuation technique for frequency measurements and comparison with the visualisation technique. The results quantify the range of application of the different techniques, and include an analysis of the liquid disintegration process as function of the liquid velocity when exposed to different air flow velocities, along with the quantification of break-up lengths, disintegration frequencies and spray angles, and show that the disintegration of the liquid sheet is associated with a periodic process, which is mainly dependent on the absolute air velocity and the air–liquid momentum ratio. Correlations are proposed for liquid sheet break-up length and frequency based on the air-to-liquid momentum ratio.

Keywords: Liquid sheet disintegration; Visualisation; Two-phase flows; Laser attenuation technique; Frequency analysis; Break-up lengths

* Corresponding author. Tel.: +351-1831-7013; fax: +351-1831-7213.
E-mail address: icarvalho@dem.isel.ipl.pt (I.S. Carvalho).

0301-9322/02/$ - see front matter
PII: S0301-9322(01)00088-X

1. Introduction

The basic mechanisms involved in airblast atomisation have been studied for a number of years making use of planar liquid films and major achievements have been reported since Fraser et al. (1963) and Dombrowski and Johns (1963), namely by Arai and Hashimoto (1985), Mansour and Chigier (1990, 1991), Eroglu and Chigier (1991), Stapper et al. (1992), Lozano et al. (1996), Carentz et al. (1998) and Hardalupas et al. (1998), among others. These studies were conducted in quiescent ambient and/or between two co-flowing air streams. A summary of some of the most relevant studies performed in 2-D liquid films is given in Table 1. The main contribution/advantage of the present configuration is related with the possibility of on-line visual control of both liquid and air streams. This is of great importance, because it allows the visualisation of the liquid flow inside the nozzle (which is transparent), and air bubble formation can be visualised and appropriate flow regulation measurements can be performed to eliminate them. This fact also allows the minimisation of other overlapping phenomena (due to air bubble formation in the liquid) that can be misleading in the interpretation of the results for the process under study.

Analysis of the liquid disintegration process has been based on the aerodynamic interaction between liquid and air, which gives rise to the formation of waves (dilatational or/and sinusoidal) on the liquid surface, that grow up to a critical point, as illustrated in Fig. 1. Then, ligaments and/or liquid clusters separate from the liquid sheet, which subsequently fragment into droplets (Dombrowski and Johns, 1963). Those waves are characterised by a wave length, a wave amplitude rate and a frequency, which depend on the working conditions (Eroglu and Chigier, 1991; Chigier and Dumouchel, 1996). Fig. 1 illustrates these mechanisms, based upon the theoretical and experimental study of Hagerty and Shea (1955). These authors show that only two kind of perturbations may exist that can lead to the disintegration of the liquid sheet, namely: (i) a sinusoidal or non-symmetric perturbation (see Fig. 1a), where the two liquid–air interfaces oscillate in phase, and; (ii) a dilational or symmetric perturbation, characterised by not in phase oscillations. Hagerty and Shea (1955) also observed that the growth rate of the sinusoidal instabilities is always higher in comparison to that of the dilational instabilities. In consequence, more effort have been put into the study of characteristics of the sinusoidal perturbations (e.g., Chigier and Dumouchel, 1996).

Arai and Hashimoto (1985) studied a planar liquid film and report similar results for the break-up frequency, making use of strobe light illumination, and the liquid film oscillation frequency, which was measured with a laser dispersion technique. The oscillating frequency of a planar liquid film was later analysed by Mansour and Chigier (1991) and Lozano et al. (1996), for different geometries and working conditions. All these studies showed that the disintegration frequency slightly increases with the liquid velocity, but strongly increases with the air velocity. The resulting wave amplitudes and spray angles were particularly studied by Eroglu and Chigier (1991), Mansour and Chigier (1991) and Lozano et al. (1996) using several visualisation techniques, making comparisons difficult to achieve, due to the different geometrical configurations used (see Table 1). Moreover, streamwise vorticity was shown to considerably influence the break-up process (e.g., Lozano et al., 1996; Chigier and Dumouchel, 1996), but its effect on the disintegration process was not quantified in a systematic way.

Although several studies have recognised the importance of non-dimensional groups, such as the Reynolds and Weber numbers, flow phenomena inside the nozzle, turbulence of the liquid

Table 1
Summary of the main flow configurations studied

Reference	L (mm)	t_L (mm)	U_L (m/s)	m_L (g/s)	t_G (mm)	U_G (m/s)	m_G (g/s)	Comments
Rizk and Lefebvre (1980)	50	0.089*–0.400	1–5	4.5–22.7	5.50–5.65	55–120	18.6–40.68	*Studied thickness
Arai and Hashimoto (1985)	200	0.4–1.0	0.5–2.0	39.9–399.2*	**	23–67	–	*Estimated values **Not available
Mansour and Chigier (1990)	30.6	0.254*–1.450	1.5–8.0	11–63	1.450*–2.210	0–145	0–7.72	*Studied thickness
Mansour and Chigier (1991)	30.6	0.254*–1.450	0.81–16.23	6.31–126.18	1.450*–2.210	17.73–119.62	1.89–12.73	*Studied thickness
Beck et al. (1991)	**	0.102; 0.203 e 0.305	0.66*–4.9	10–25	**	13–60	3.0*–13.8	*Estimated values **Similar to Rizk and Lefebvre (1980)
Eroglu and Chigier (1991)	30.48	0.254	1.6–16.1	12.5–125	1.45	17.7–74.7	–	Similar to Mansour and Chigier (1991) experimental set up
Stapper et al. (1992)	47	0.508	1–5	23.9–119.4	3.7*	0–60	0–126**	*Estimated values **Maximum possible value
Lozano et al. (1996)	80	0.95	0.2–2.45	15–186	10	8–65	8–62.4	–
The present case	80	0.7	0.6–6.4	30.6–359.0	7	0–40	0–36	Transparent nozzle Independent air velocity control

L: liquid film length, U_L: liquid film velocity at injector tip, U_G: air stream mean velocity, t_L: liquid film thickness, t_G: air film thickness, m_L: liquid mass flow rate, m_G: air mass flow rate.

film, the balance of axial and radial components of the liquid velocity, existence of primary disturbances and/or order of magnitude of relative velocities (Dombrowski and Johns, 1963; Lee, 1985; Mansour and Chigier, 1991; Stapper et al., 1992), there is no clear explanation of the dominant cause for liquid disintegration. It is, nevertheless, recognised that all these mechanisms are connected with wave formation, wave development and wave disintegration, the break-up length being mainly dependent on the growth rate of the wave itself. The wave amplitude increases with the distance from the nozzle, but the spatial amplitude growth rate decreases with liquid mass flow rate and increases with the air velocity (Eroglu and Chigier, 1991; Chigier and Dumouchel, 1996). High spatial amplitude growth rates occur for low liquid mass flow rates. The disturbances are known to be amplified faster when the aerodynamic force increases at the air/liquid interface due to higher relative velocities.

Although a range of tests in axisymmetric geometries have been reported in literature (Adzic et al., 1994; Carvalho and Heitor, 1997; Karl et al., 1996), the particular complexity of the airblast geometry requires fundamental studies on planar liquid sheets. In this context, the present paper is aimed to improve on understanding of the periodic nature of the liquid break-up process and assess the use of optical diagnostics for this purpose.

The present work involves the analysis of the flow downstream a 2-D planar liquid film surrounded by two independently controlled air flows, and follows the previous reported work

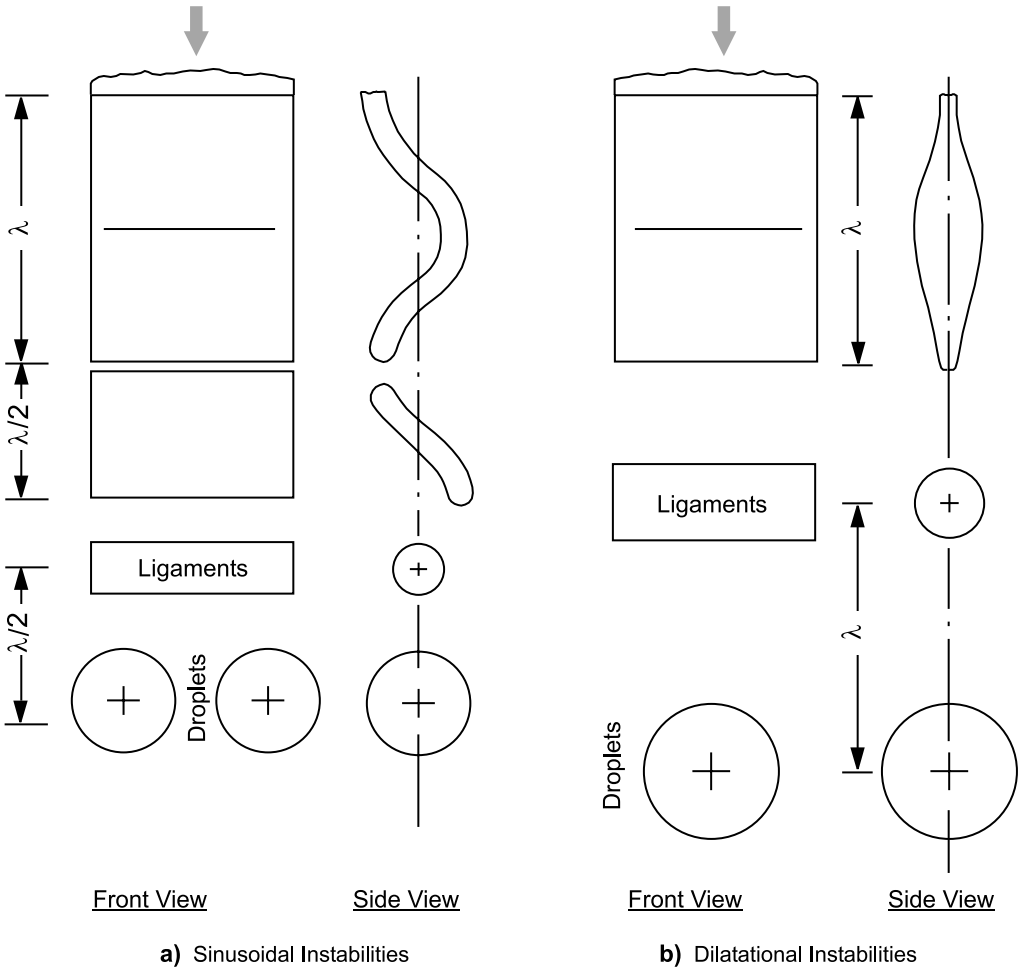

Fig. 1. Instability types that can exist in a liquid film disintegration process.

(Carvalho et al., 1997a,b, 1998). The ultimate objective is to improve knowledge of the liquid break-up mechanisms and their relation with the atomisation quality in airblast nozzles of practical relevance. In this context, this paper also aims to discuss and compare two different experimental techniques for the frequency analysis of the disintegration process, and two visualisation techniques for wave amplitude and spray angle measurements.

Section 2 describes the flow configuration and the experimental techniques used throughout the work. Section 3 presents and discusses the results and the main findings are summarised in Section 4.

2. Experimental method: liquid film generator and instrumentation

Fig. 2 shows a schematic diagram of the liquid film generator along with the instrumentation used. The 2-D liquid film generator consists of: (i) an inner liquid flow, with an exit thickness of

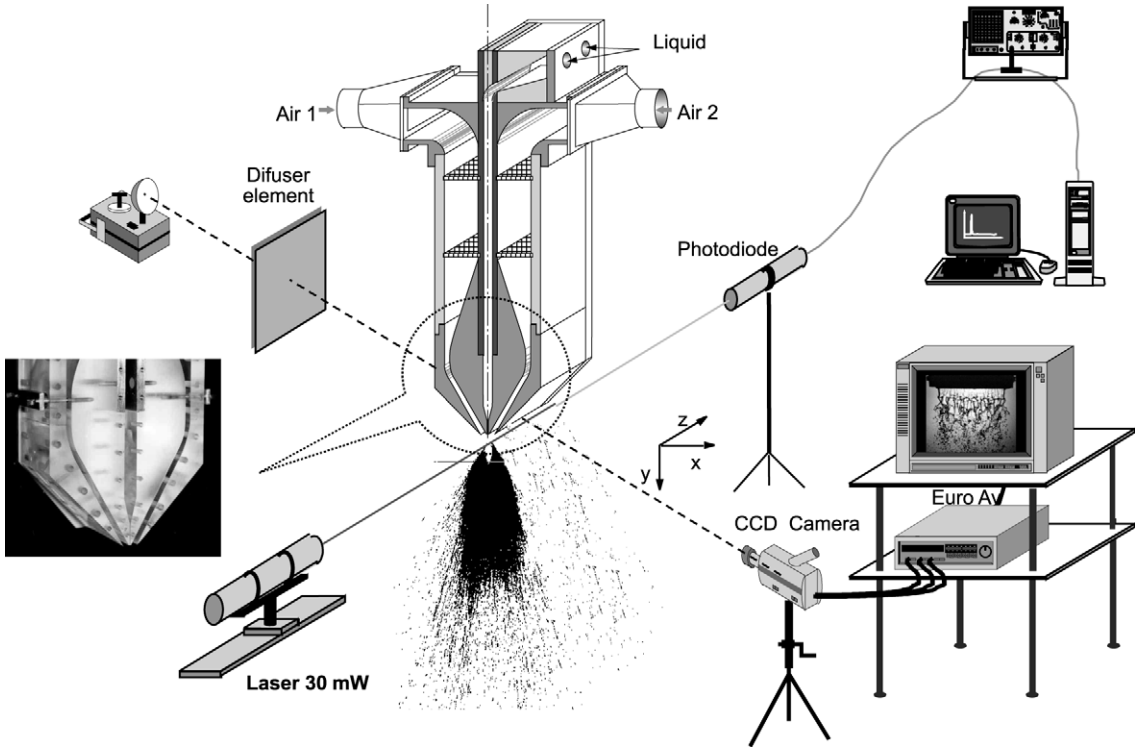

Fig. 2. Schematic diagram of the flat liquid film generator and experimental techniques configuration.

$t_L = 0.7$ mm, and an aspect ratio of $L/t_L = 114$, that is, 80 mm wide; and, (ii) two co-current air flows, with a thickness $t_G = 7$ mm, which are passed along both sides of the liquid film to produce a shear force at the air–liquid interface. Air can be fed through the left and right channels separately, thus allowing the air velocity ratio to be varied between 1 and 4, with absolute average velocities up to 39 m/s ($Re_G = (\rho_G U_G t_G)/\mu_G \leqslant 17\,647$). The impingement angle of the air flows towards the liquid film is 30°. Water was used as the test liquid, and the results reported here are for a liquid velocity between 0.7 and 6.4 m/s ($543 \leqslant Re_L = (\rho_L U_L t_L)/\mu_L \leqslant 4963$).

Different visualisation techniques were used throughout the work, which include laser light sheet illumination obtained by spreading a laser beam with a cylindrical lens, with individual images acquired by a 35 mm camera operating with 400 ASA films, and exposure time varying between 4 and 66 ms. In addition, strobe light visualisation was used and flow images were acquired by a CCD video camera, each frame corresponding to an individual image of the flow, with an exposure time of 1.2 μs. These techniques allowed the quantification of spray angles, wave amplitudes, and break-up lengths and frequencies. The break-up frequency of the liquid sheet was analysed by matching the strobe light frequency, f_s, with that of the flow, following the work of Arai and Hashimoto (1985). These authors studied the disintegration of a liquid film, measuring break-up lengths and wave amplitudes by means of photography, and break-up frequency and oscillation frequency using strobe light matching and laser light attenuation techniques, respectively. Their study made available two empirical correlations: one for the break-up length and another for the break-up frequency.

Frequency measurements were also performed by means of a laser light beam (He–Ne laser, 30 mW), positioned parallel to the flow in a 180° arrangement with a photodiode which generates a current proportional to the incident light intensity, which varies as the liquid film crosses the laser light beam, and causes its attenuation (Arai and Hashimoto, 1985; Mansour and Chigier, 1991). For the results presented here, the system is located in the break-up region, previously assessed by the strobe light visualisation technique. The current of the photodiode is converted into voltage, which was in turn fed to a digital oscilloscope to visualise the waveform, and simultaneously transferred to a PC, and a Fourier analysis was performed to determine the dominant frequencies. In each point 10 series of 16 304 points were acquired, with an acquisition rate of 20 kHz, and individually submitted to a Fourier analysis (Fernandes and Heitor, 1997), which gives us the mean power spectra, where dominant frequencies (higher energy) plus its harmonics can be identified. As previously reported by Arai and Hashimoto (1985), the break-up frequency was seen to be coincident with the oscillating frequency of the liquid film, prior to disintegration.

Frequency measurements show that the frequency is not dependent on either the axial or radial measurement locations. In the presence of the flow, the SNR is good. The control volume position inside the flow does not affect the dominant frequency, as previously observed by Mansour and Chigier (1991). The SNR is dependent on the control volume position, in a way that it is minimum in the plane of the liquid film (higher attenuation) and maximum in the outer regions ($\approx$1 mm off axis).

3. Results and discussion

The results of the work discussed in this paper are presented in three parts, namely: (i) spray angles; (ii) break-up frequencies; and, (iii) break-up lengths of the liquid sheet. First, for a better overall evaluation of the referred flows, extended visualisation results will be shown, both front and side views, for different experimental techniques, namely, strobe light illumination and laser light sheet visualisation.

3.1. Visualisation results

Fig. 3 presents sample results of two different views of the liquid film for different air mass flow rates, and $U_L = 0.7$, 1.3, 1.6, 1.8, 2.1, 2.5, 2.9, 3.4, 4.3 and 6.4 m/s. The air velocity ratio is kept constant and equal to unity, and the absolute air velocities are $U_G = 0$, 15, 20, 30 and 39 m/s.

Fig. 3a presents front views of the flat liquid film obtained in the absence of air ($U_G = 0$), and shows a convergent liquid sheet bounded by thick rims that are drawn together by surface tension forces, as first described by Mansour and Chigier (1990). The convergence length, L_c, increases with the liquid film velocity, U_L. Although the present results must be extrapolated with care, due to their dependence on the geometry of the sheet generator, they show a clear linear increase of the convergence length as the liquid flow rate increases, which is in qualitative agreement with the results of Mansour and Chigier (1990). For the present case it is verified that $L_c = 78.6U_L + 11.5$, with a correlation coefficient of 0.999. Representing the results in a non-dimensional form, using L_c/t_L and $Re_L = (t_L U_L/v_L)$ as dimensionless groups for L_c and U_L the results of both studies follow

the curve $L_c/t_L = 0.15Re_L + 6.72$, with a correlation coefficient of 0.996. The central part of the film keeps a smooth appearance for low liquid velocities, U_L. Small ripples start to appear in the centre of the liquid film for $U_L \geqslant 2.1$ m/s ($Re_L = 1628$). As the liquid mass flow rate increases, this effect is more pronounced and at $U_L = 2.9$ m/s ($Re_L = 2249$) the liquid surface becomes clearly disturbed over all its extension, following again Mansour and Chigier (1990). These disturbances are damped on the downstream region, because turbulent energy production ceases at the nozzle exit and the liquid sheet tends to laminarize as a result of viscous dissipation of turbulent energy.

In Fig. 3b and c (which provide front and side views), the liquid film behaviour, when surrounded by two air flows, can be observed. The characteristic of these flows resembles those

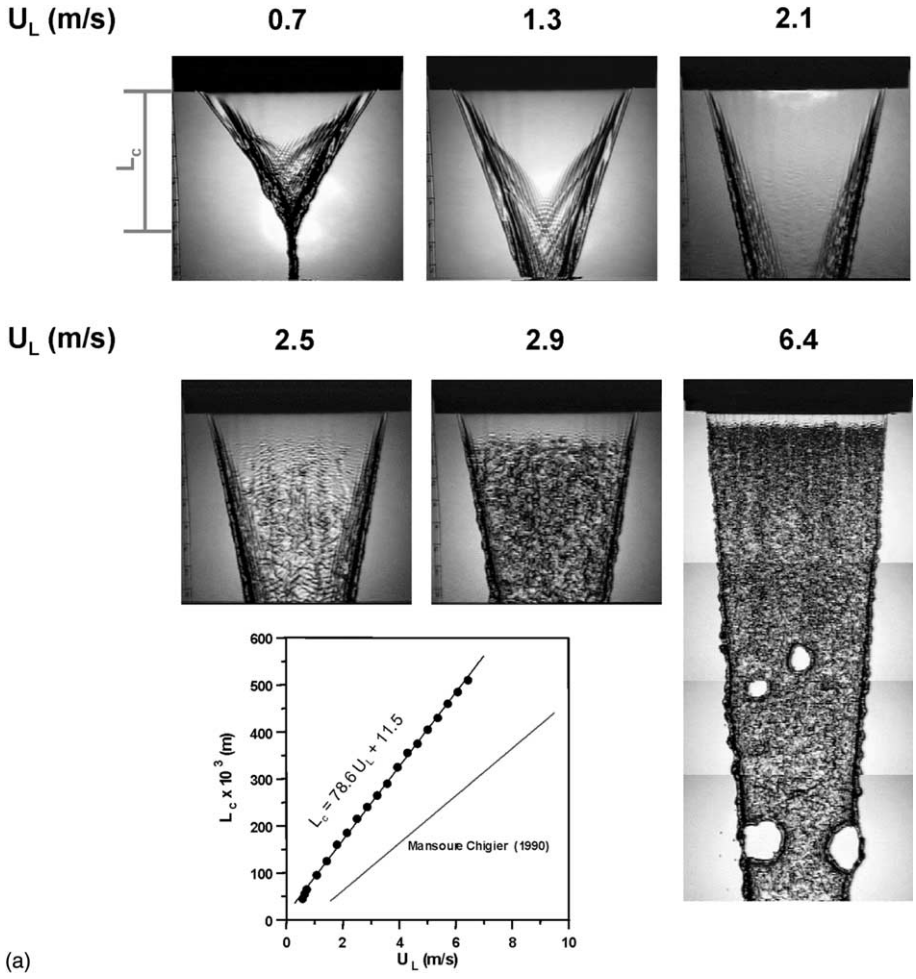

Fig. 3. Visualisation of the flat liquid film for different liquid and air velocities: (a) front view of the liquid film in the absence of air, using strobe light illumination, (b) front view and side view of the liquid film for $U_G = 15$ m/s and $U_G = 39$ m/s, using strobe light illumination, (c) side view of the liquid film for $15 \leqslant U_G$ (m/s) < 39, using laser light sheet illumination.

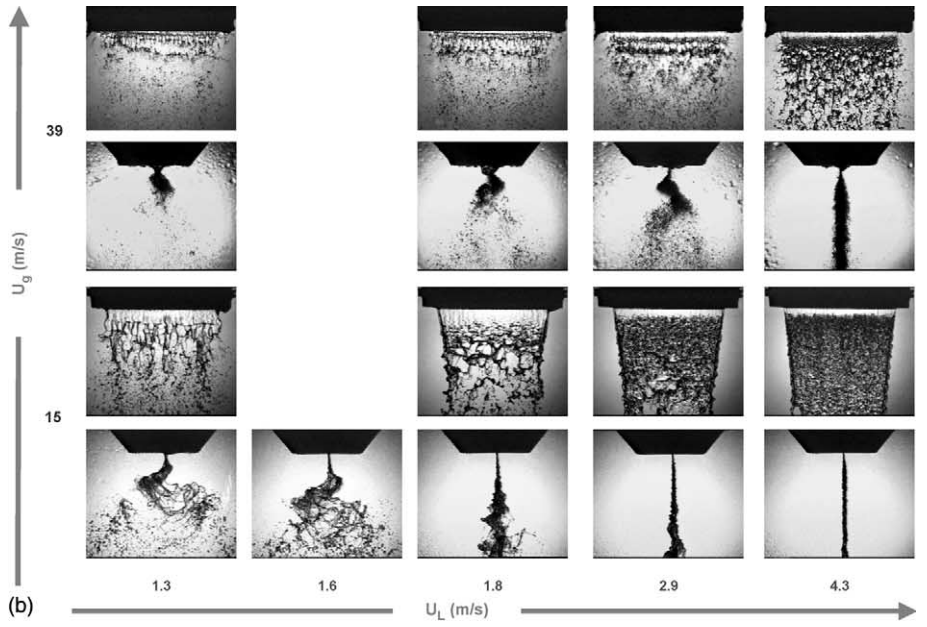

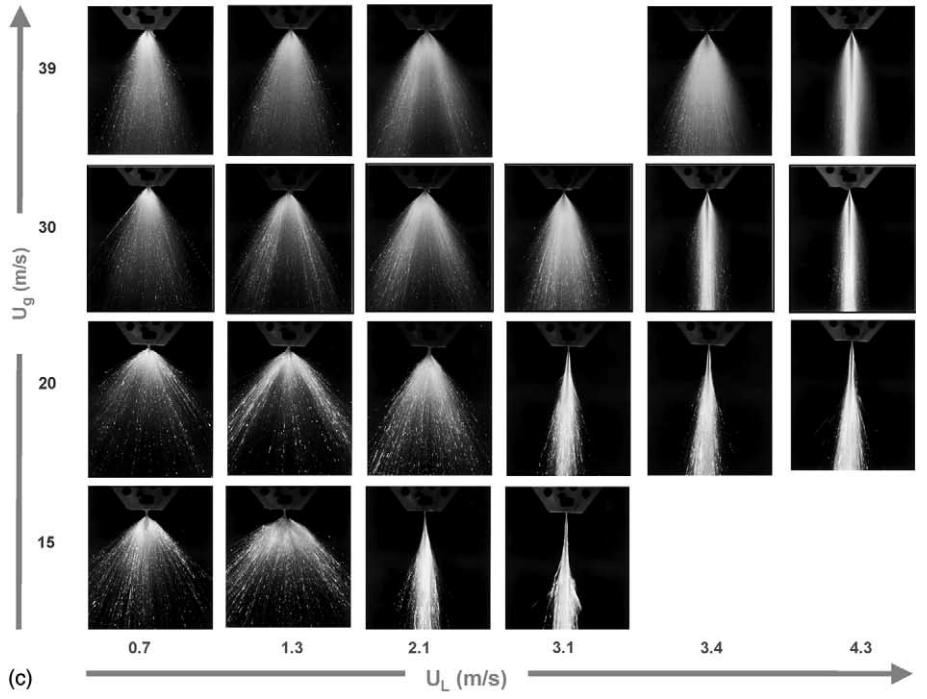

Fig. 3. (*continued*)

obtained by Mansour and Chigier (1991) and Lozano et al. (1996), and we can see the cellular type of structures (well organised), and the streamwise ligaments which are formed very close to the nozzle exit. All the results are in agreement with previously obtained ones, although attention should be drawn to the fact that the geometrical configuration plays an important role in this type of phenomena, affecting the mixing process between the two fluids, as in the present configuration the atomising air has a radial velocity component towards the liquid film, which as a consequence, enhances the interaction between the two fluids, as previously referred by Lefebvre (1992). This is one of the reasons why comparison and extrapolation of the present results and the ones obtained in previous studies reported in literature, must be carefully performed.

In the disintegration of the liquid film, the formation of a surface wave is one of the recognised important factors contributing to the break-up phenomena. The wave formation may be caused by Kelvin–Helmholtz instability due to the liquid/air interaction (Faragó and Chigier, 1992). Disintegration occurs when the wave amplitude reaches a critical value, as previously described by Dombrowski and Johns (1963), and fragments of the liquid are torn off from the "outer layers" of the liquid film.

As the liquid velocity decreases, the sheet gives rise to streamwise ligaments, which are formed very close to the nozzle. The analysis shows that a spanwise wave is superimposed on top of the streamwise ligaments, which grow together and, as a result, give rise to the type of distorted waves described by Mansour and Chigier (1991) downstream of the initial sinusoidal wave. The present liquid film behaviour is consistent with the results from Arai and Hashimoto (1985), Lee and Wang (1986) and Eroglu and Chigier (1991).

The presently studied atomisation process is mainly driven by the energy transfer from the air streams to the liquid film. The present work shows that the amount of energy transferred from the air to the liquid has a "critical value" for which the atomisation quality suffers an abrupt increase (referred to as "transition" points). A parameter that allows the characterisation and prediction of the transition points of the liquid film disintegration mode is the air-to-liquid momentum ratio, defined as $\mathrm{MR} = \rho_G U_G^2 / \rho_L U_L^2$.

For low air-to-liquid momentum ratio the dilatational wave dominates the liquid film disintegration mode. The atomisation quality is rather poor and a narrow spray angle is obtained (e.g., $U_G = 15$ m/s and $U_L \geqslant 1.8$ m/s). For higher air-to-liquid momentum ratios, the sinusoidal waves dominate, and the atomisation quality is considerable improved, as the spray angle increases significantly (e.g. $U_G = 39$ m/s and $U_L \leqslant 3.9$ m/s). The above-mentioned working conditions define the "transition" flows, and the air-to-liquid momentum ratio value that characterises this transition is about 0.5. For considerably higher air-to-liquid momentum ratios, namely with low liquid velocities or high air velocities (e.g., $U_G = 15$ m/s and $U_L \leqslant 0.7$ m/s; or $U_G = 39$ m/s and $U_L \leqslant 2.9$ m/s), the liquid film emerging from the nozzle is rapidly torn into small fragments by the immediate interaction between the liquid and the impinging air streams, as already suggested by Lefebvre (1992). For considerably low air-to-liquid momentum ratios, namely for high liquid velocities or low air velocities (e.g., $U_G = 15$ m/s and $U_L \geqslant 4.3$ m/s) no wave was seen to be present in the liquid surface.

The analysis of all the visualisation results, plus the quantification of the "transition" disintegration processes, is also observed by the quantification of spray angles, frequencies and break-up lengths, as discussed in the following section, which gives further insight into some of the studied flows, and provides empirical correlations for frequency and break-up lengths.

3.2. Spray angles, frequencies and break-up lengths measurements

3.2.1. Instability amplitudes and spray angles

The spray angle measurement is a form of evaluating the amplitude of the liquid sheet instability, as the former is closely dependent on the latter. The critical amplitude of the instabilities for which the break-up occurs determines the angle of the spray and several techniques can be used to measure these characteristics (e.g., Mansour and Chigier, 1990, 1991; Lozano et al., 1996). In the present work two different visualisation techniques are used: laser light sheet illumination and strobe light illumination.

Fig. 4a shows the results obtained for $U_G = 15$ and 30 m/s with laser light sheet and back light illumination, with a strobe light, for $U_L = 1.3$ m/s. In the case of the laser light sheet illumination, the spray angle is measured making use of a visually observed average value of contrast between the "white" spray and the "black" background. For the back light illumination the criteria was to follow the crests of the major disturbances. The surrounding droplet mist was not generally considered. In both cases the uncertainty of the measurements is estimated to be 5%.

Fig. 4b shows the results obtained with both techniques for $U_G = 30$ m/s. It is observed that the results obtained with the laser light sheet are 40% higher, when compared with the back light illumination technique. This is related with the exposure time used, which was about 33 ms for the laser light sheet, and between 1.2 and 0.8×10^{-3} ms for the back light illumination. In addition, the differences observed are also related to the droplet mist that surrounds the "wave crests" (see Fig. 4a1 and a3), which is not considered for spray angle measurements in the back light illumination, and is obviously accounted for with the laser light sheet technique. When comparing both techniques, it is observed that the values obtained with the laser light sheet a more accurate quantification of the spray angle, and that the back light illumination technique is more adequate for instability amplitude measurements. This is due to the fact that, spray angle measurements require some level of temporal integration, as those provided by the laser light sheet technique.

Fig. 4c shows measured spray angles making use of the laser light sheet technique. For all operating conditions, regardless the air velocity, a region of maximum spray angle occurs, followed by a sharp decrease for higher values of liquid velocity. The maximum values of the spray angle (e.g., for $U_G = 15$ m/s the maximum angle is observed at $U_L = 1.3$ m/s) are displaced for higher values of liquid velocity as the air flow rate increases (e.g., for $U_G = 30$ m/s the maximum angle is observed at $U_L = 1.8$ m/s), the maximum value decreasing with air flow rate, as easily seen in Fig. 3c and d. For example, it was observed that for $U_G = 15$ m/s the region corresponding to the sharp decrease of the spray angle (i.e., the "transition flow") appears for a specific liquid velocity value, as illustrated in Fig. 2d. Compare, for example, in Fig. 3d, at $U_G = 15$ m/s the characteristics of the flows with $U_L = 1.3$ and 2.1 m/s. The transition flow is characterised by a spray angle oscillation in a range of about 15–20°. For a small increase in the liquid velocity, very poor atomisation is obtained and the spray angle assumes very small values. Also, for higher air flow velocities the spray angle decrease becomes less sharp, when the liquid velocity increases (see, e.g., sequences for $U_G = 15$ and 30 m/s in Fig. 3c and d).

3.2.2. Break-up frequencies

For break-up frequency measurements two different techniques are used: strobe light with variable frequency illumination and laser light attenuation. Fig. 5 shows results for the two

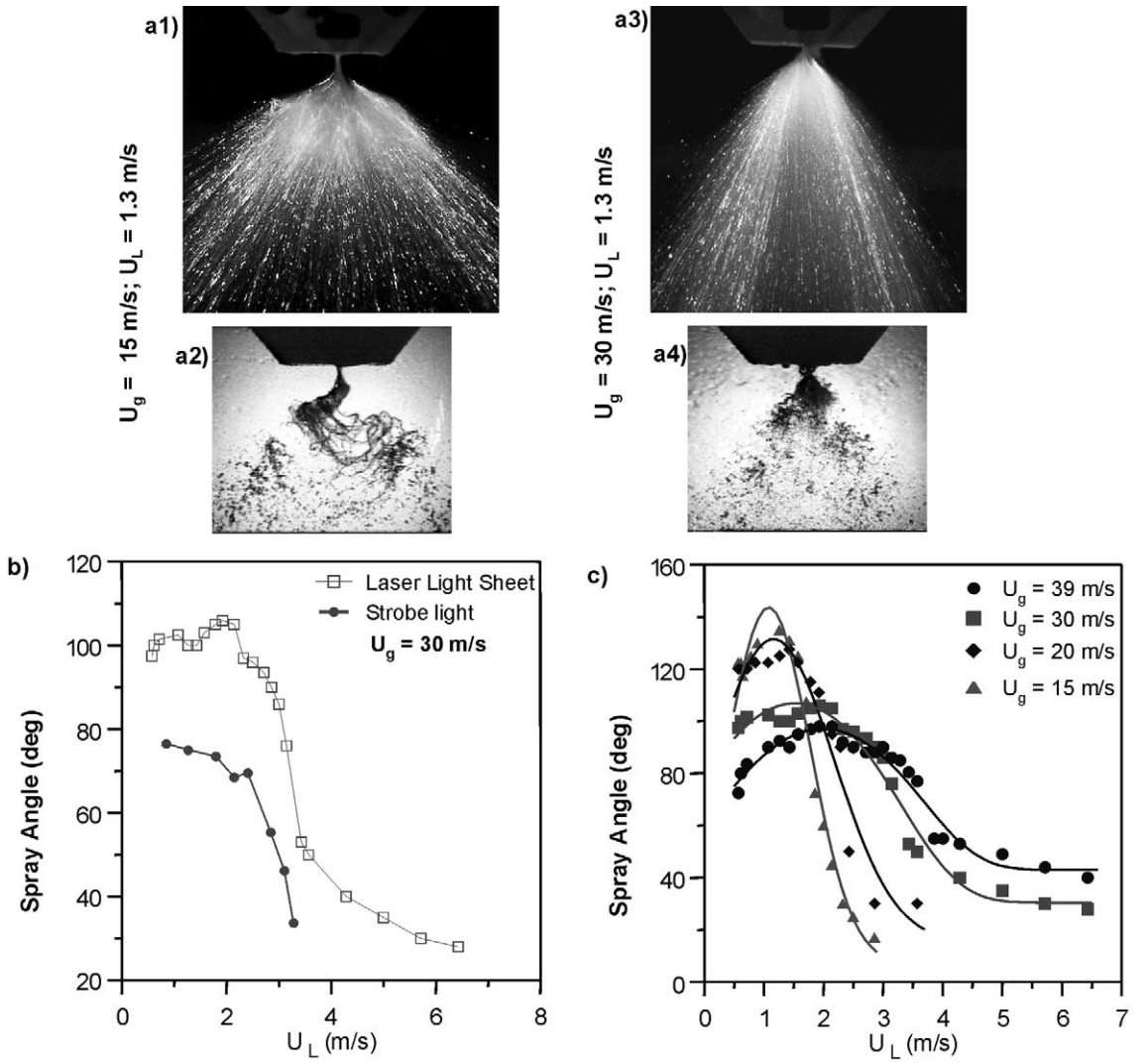

Fig. 4. Spray angles as function of liquid velocity: (a1–a4) Side views of the liquid film using strobe light and laser light sheet illumination, (b) spray angles as function of liquid velocity for $U_G = 30$ m/s and for the two different techniques, (c) spray angles as function of liquid film for $15 \leqslant U_G$ (m/s) < 39, using laser light sheet visualisation.

techniques for $U_G = 15$ m/s, along with three typical power spectrum for different liquid velocities (see Fig. 5b–d), together with the electronic noise, which can be observed in the log–linear representation, in Fig. 5c. A fixed noise frequency at 286 Hz, due to the acquisition board itself, is always present. The peak corresponding to that frequency does not affect the frequency analysis presented here. In Fig. 5a the power spectrum for $U_G = 15$ m/s and $U_L = 0.7$ m/s is shown in a linear scale. This figure clearly shows the fundamental frequency at $f = 119$ Hz, by its maximum power. In Fig. 5c the fundamental frequency for $U_L = 1.5$ m/s can be identified at $f = 138$ Hz. Additionally, the log–linear representation of the power spectrum allows the identification of the

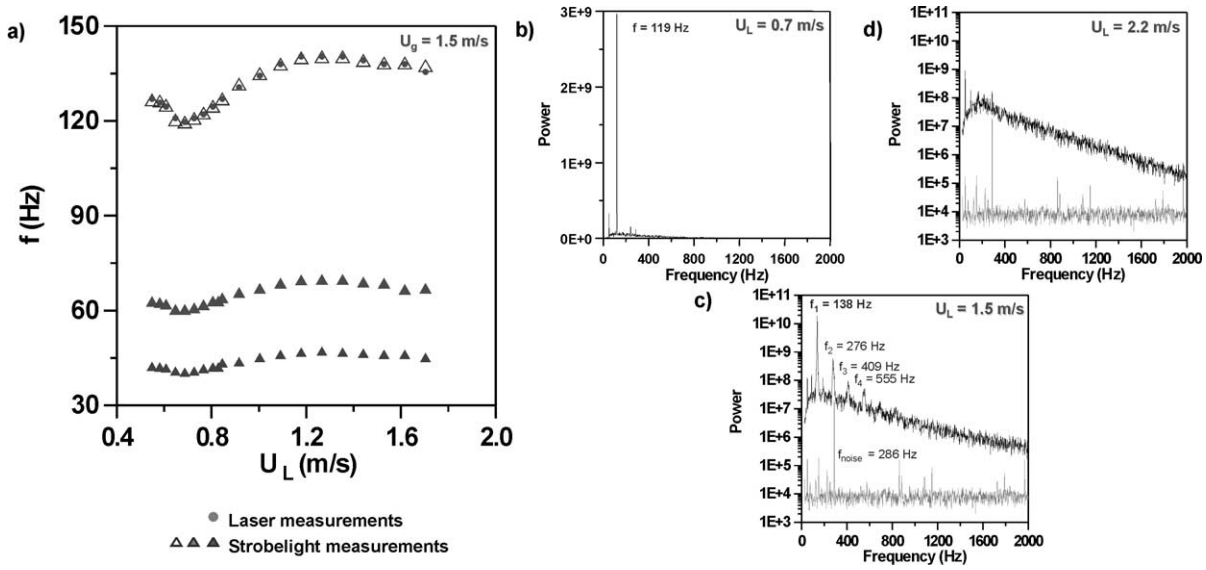

Fig. 5. Break-up frequency of the liquid sheet: (a) as a function of the liquid velocity for $U_G = 15$ m/s, (b) corresponding power spectrum obtained for $U_L = 0.7$ m/s, (c) corresponding power spectrum obtained for $U_L = 1.5$ m/s, (d) corresponding power spectrum obtained for $U_L = 2.2$ m/s.

harmonic frequencies $(f_n = nf)f_2 = 276$ Hz, $f_3 = 409$ Hz and $f_4 = 555$ Hz. The frequencies below the fundamental one correspond to the electrical net noise at 50 Hz and to a subharmonic.

The axial position of the control volume determines the ''meaning'' of the measured frequency. If it is positioned upstream of the break-up region, an oscillating frequency is measured, while the results of the break-up frequency are obtained when the control volume is located downstream of that region. As the fundamental frequency does not depend on the axial position, it is assumed that the break-up and the oscillating frequencies are equal. This conclusion is also supported by the comparison between the results obtained with the different frequency measuring techniques, as shown in Fig. 5a. As referred before, the strobe light technique allows the ''freezing'' of the break-up phenomena for different frequency values. Three different measurements were always recorded for each operating condition, and three curves were obtained as shown in Fig. 5a. On the other hand, the laser attenuation technique allowed the identification of the fundamental frequency, and the results show maximum relative deviations between the values measured with two techniques below 3%.

Based on the strobe light measurements, the wave frequencies, f, for several air velocities are plotted in Fig. 6a, as a function of the liquid velocity. The dashed lines plotted here, represent different regions defined in previous works performed by Chigier and co-workers, and correspond to different disintegration modes (A, B and C). An overall appreciation of the results shows that the wave frequency increases with liquid flow rate and also with air velocity. At low liquid flow rates (region A) the energy transferred by shear is sufficient to lead to sinusoidal mode oscillations, with long wavelengths or low frequencies. In region B, we have a combined mode oscillation: sinusoidal and dilational (Mansour and Chigier, 1991). As the liquid flow rate increases, the dilational mode becomes more and more important and the frequency still increases with U_L. The

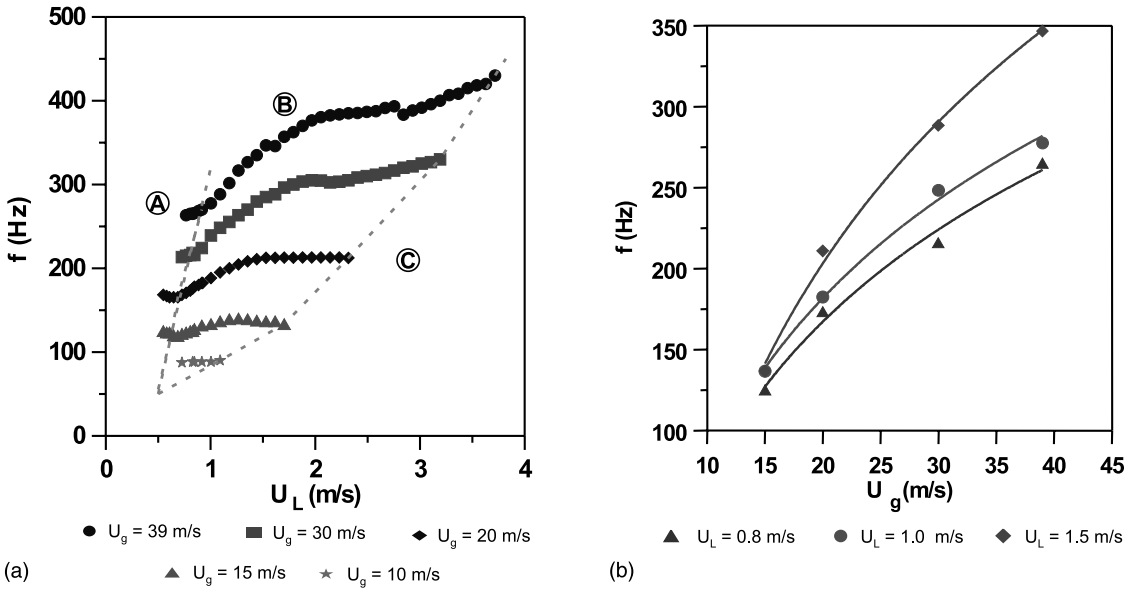

Fig. 6. Break-up frequency of the liquid sheet: (a) as a function of the liquid velocity, (b) as function of air velocity.

"plateau" is observed for all flows with the onset of the maximum spray angle, that is, after that point the sinusoidal mode is still present, but the dilational mode begins to have a stronger influence. The transition to region C corresponds to the onset of a dominant dilational mode (Mansour and Chigier, 1991), always present for high values of U_L, where not enough energy is transferred to the liquid film due to air interaction, and corresponds to the onset conditions of the "transition" flow. In this region, no dominant frequency was identified. With the strobe light it is no longer possible to "freeze" the flow, and the power spectrum obtained with the laser attenuation technique does not allow the identification of a fundamental frequency due to the total widening of the bandwidth of frequency peaks, as shown in Fig. 5d. The peak with higher energy in this spectrum corresponds to the electrical net noise at 50 Hz followed by the electronic noise of the acquisition board at 286 Hz.

Also shown in Fig. 6b is the influence of the air velocity on the liquid film disintegration frequency, for $U_L = 0.8$, 1.0 and 1.5 m/s. The oscillation frequency is strongly dependent on U_G, with $f \propto U_G^{0.73}$, $f \propto U_G^{0.70}$ and $f \propto U_G^{0.88}$, for $U_L = 0.8$, 1.0 and 1.5 m/s, respectively.

3.2.3. Break-up lengths

The break-up length, defined as the distance between the injector tip and the horizontal plan were the film break-up first occurs, was measured by means of the images obtained with back light illumination.

Fig. 7a shows sample front views of the flows, with $U_G = 15$ m/s and different liquid velocities, allowing a better insight into the break-up process, as well as the way the break-up lengths are defined for different operating conditions. Fig. 7b shows the break-up length, L_b, as a function of the liquid velocity, U_L, for different air velocities. As the coflowing air streams result in an

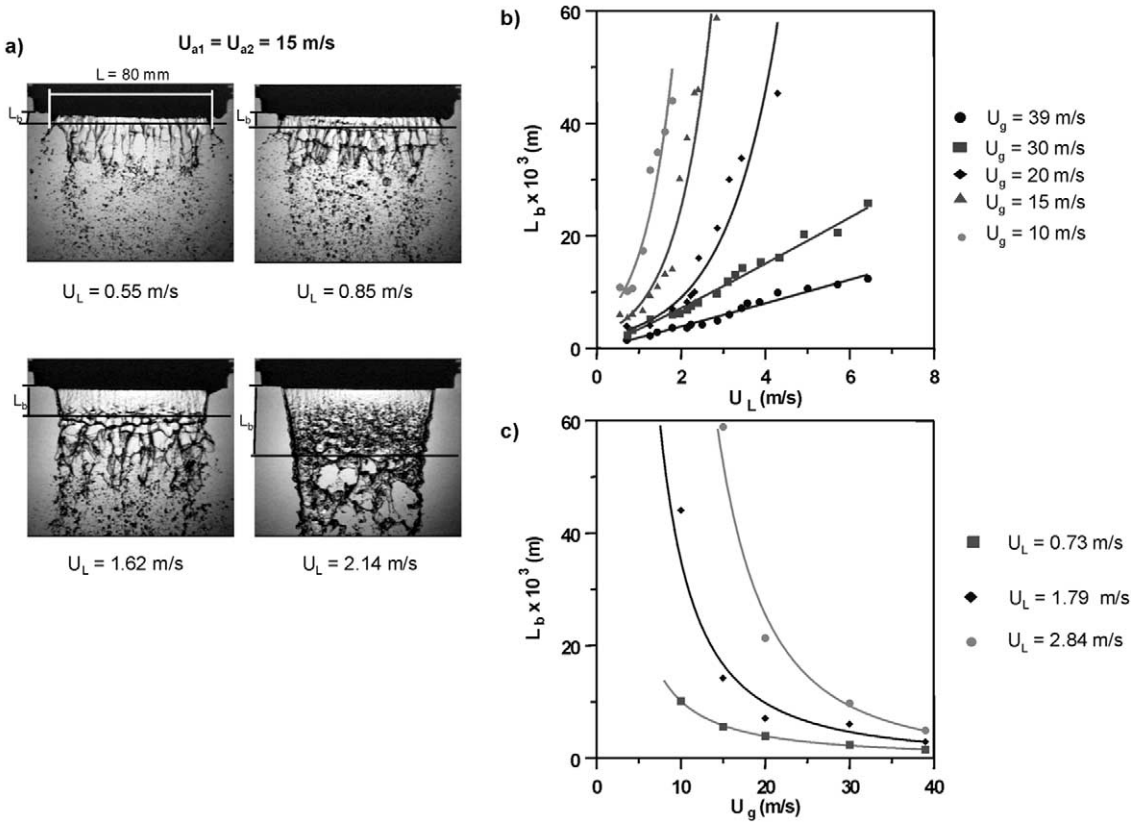

Fig. 7. Break-up length of the liquid sheet: (a) representation of the break-up length measurement, (b) break-up length as function of the liquid velocity, (c) break-up length as function of the air velocity.

acceleration of the liquid film layers, the break-up length increases with the liquid velocity and decreases with the air flow rate, independently of its magnitude.

Also shown in Fig. 7c is the influence of the air velocity on the liquid film break-up length, for $U_L = 0.73$, 1.79 and 2.85 m/s. The break-up length is strongly dependent on U_G, with $L_b \propto U_G^{-1.39}$, $L_b \propto U_G^{-1.85}$ and $L_b \propto U_G^{-2.51}$, for $U_L = 0.73$, 1.79 and 2.85 m/s, respectively.

As visualisation results have been widely represented and analysed in detail, it is now necessary to move forward to a joint analysis of the above presented results, mainly break-up frequencies and break-up lengths, in order to be able to present the proposed correlations, for the different parameters under study.

3.2.4. Joint analysis and proposed correlations

Although the importance of certain non-dimensional groups, as the Reynolds and Weber numbers, is well established (Arai and Hashimoto, 1985; Eroglu et al., 1991; Chigier and Reitz, 1996), the relative weight of the different non-dimensional groups was evaluated, and the importance of the air-to-liquid momentum ratio, MR, was noticeable. As it is, a better correlation

can be obtained between all the studied flow conditions, if the momentum ratio group, MR, is considered.

A non-dimensional break-up length, L_b/t_L, was chosen (Stapper et al., 1992; Lozano et al., 1996). Although it is common to find, in the literature, the break-up frequency represented as function of the liquid velocity (Mansour and Chigier, 1991; Eroglu and Chigier, 1991; Lozano et al., 1996) a non-dimensional frequency, is defined here as ft_L/U_L, which represents the ratio between the transversal and the axial liquid velocity (as well as in accordance to the Strouhal number).

Fig. 8 shows the non-dimensional break-up length, L_b/t_L, and frequency, ft_L/U_L, as a function of, $MR = \rho_G U_G^2/\rho_L U_L^2$, the non-dimensional group that is found to control the disintegration process. The non-dimensional group, MR, provides a good correlation for the different flow conditions. Non-log representation of these results shows that, there is a sharp decrease of the break-up length until $MR = 0.5$, and for higher values of MR, L_b tends to be less dependent of this parameter. For all the studied air velocities the break-up length is related with the air-to-liquid momentum ratio by $L_b/t_L = 6.51MR^{-0.68}$, with a correlation coefficient of 0.804. As for the non-dimensional frequencies, shown in Fig. 8b, the air-to-liquid ratio is seen to be an important governing parameter, and is related with the break-up frequency by $ft/U_L = 0.13MR^{0.38}$, with a correlation coefficient of 0.965. The lower correlation coefficient obtained for the break-up length correlation is probably due to the higher uncertainty in the break-up length measurements, but can also be due to the need of considering additional parameters in future studies and analysis.

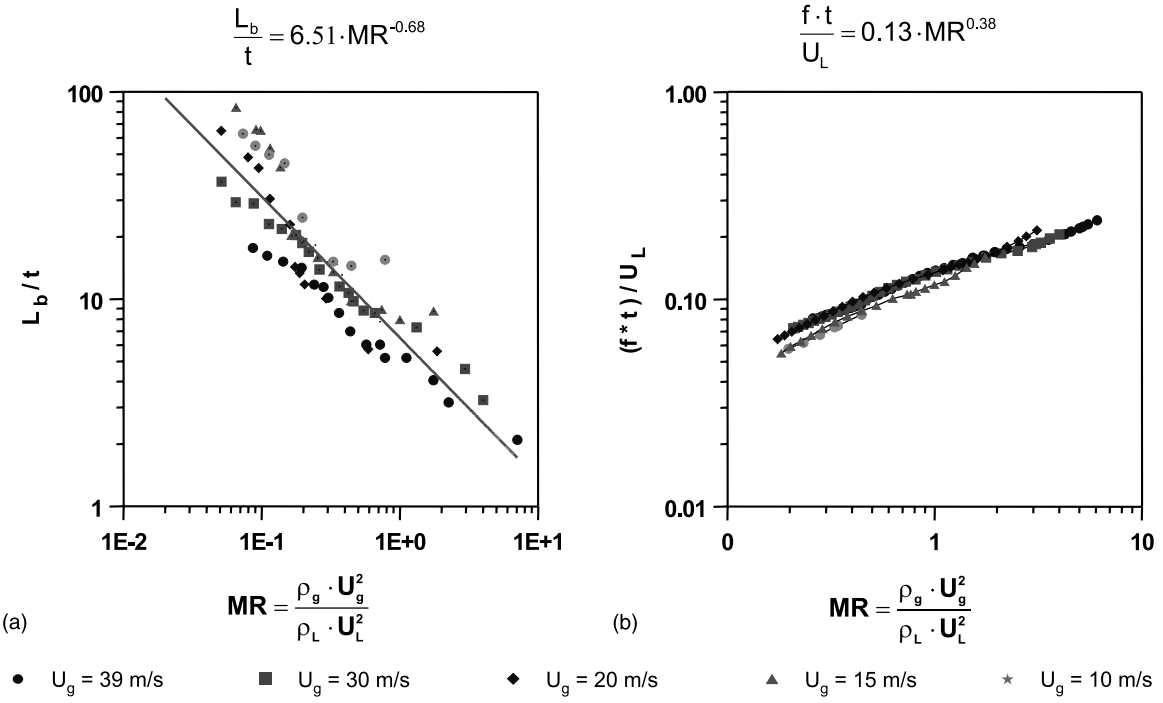

Fig. 8. Non-dimensional break-up length and frequency as function of the air-to-liquid momentum ratio: (a) L_b/t versus MR, (b) ft/U_L versus MR.

4. Conclusions

The process of liquid film disintegration into a spray is studied, making use of a 2-D liquid film surrounded by two air streams, using two different visualisation techniques and through the quantification of instability amplitudes, break-up lengths and break-up frequencies.

The visualisation results, extensively presented in this paper, compare fairly well with the ones previously presented in literature and allowed a "good" description of the disintegration process of the 2-D liquid film studied.

Despite the traditionally used non-dimensional groups in this type of studies, namely the liquid Reynolds number and gas Weber number, an extended analysis of the non-dimensional breakup lengths and break-up frequencies showed the importance of the air-to-liquid momentum ratio group, MR, as the parameter that allows to correlate the present results. The MR is an "always present" parameter independently of the operating flow conditions. A better correlation is obtained for break-up frequencies ($ft/U_L = 0.13\mathrm{MR}^{0.38}$), when compared with the one obtained for the break-up length ($L_b/t = 6.51\mathrm{MR}^{-0.68}$). This is probably due to the higher uncertainty in the break-up length measurements, but can also be due to the need of considering additional parameters in future studies and analysis.

Worth mentioning is the fact that the present nozzle configuration was made transparent in order to minimise other overlapping phenomena (due to air bubble formation in the liquid) that can be misleading in the interpretation of the results for the process under study.

Acknowledgements

Financial support has been provided through the BRITE/EURAM programme of the European Commission under the contract AERO-CT95/0122. The authors are pleased to acknowledge the research grant of Dina Santos from the PRAXIS XXI program of the Portuguese Ministry of Science and Technology.

References

Adzic, M., Carvalho, I.S., Heitor, M.V., 1994. Laser shadowgraphy of break-up of a liquid sheet downstream of a model prefilming airblast atomizer. 7th International Symposium on Applications of Laser Anemometry to Fluid Mechanics, 11–14 July, Lisbon, Portugal.

Arai, T., Hashimoto, H., 1985. Disintegration of a thin liquid sheet in a cocurrent gas stream. ICLASS-85, Paper VIB/1, 9–10 July, London, UK.

Beck, J.E., Lefebvre, A.H., Koblish, T.R., 1991. Airblast atomization at conditions of low air velocity. J. Propulsion, 207–212.

Carentz, H., Berthoumieu, P., Lavergne, G., 1998. Study of planar liquid sheet disintegration. ILASS-Europe'98, 6–8 July, Manchester, England, pp. 13–17.

Carvalho, I.S., Heitor, M.V., 1997. Liquid film break-up in a model of a prefilming airblast nozzle. Exp. Fluids 24, 408–415.

Carvalho, I.S., Heitor, M.V., Santos, D., 1998. Liquid film disintegration mechanisms. Third International Conference on Multiphase Flow, ICMF'98, 8–12 June, Lyon, France.

Carvalho, I.S., Heitor, M.V., Santos, D., 1997a. Disintegration mechanisms in flat and annular liquid films. 13th Annual Conference on Liquid Atomization and Spray Systems, 9–11 July, Florence, Italy.

Carvalho, I.S., Heitor, M.V., Santos, D., 1997b. On the analysis of shear-driven liquid break-up processes. Proceedings of the 11th Symposium on Turbulent Shear Flows, 8–11 September, Grenoble, France, pp. 27.6–27.11.

Chigier, N., Dumouchel, C., 1996. Atomization of liquid sheets. In: Recent Advances in Spray Combustion: Spray Atomization and Drop Burning Phenomena, Vol. I. Prog. Astronaut. Aeronaut. 166, 241–259.

Chigier, N., Reitz, R.D., 1996. Regimes of jet breakup and breakup mechanisms (physical aspects). In: Recent Advances in Spray Combustion: Spray Atomization and Drop Burning Phenomena, Vol. I. Prog. Astronaut. Aeronaut. 166, 109–136.

Dombrowski, N., Johns, W.R., 1963. The aerodynamic instability and disintegration of viscous liquid sheets. Chem. Eng. Sci. 18, 203–214.

Eroglu, H., Chigier, N., 1991. Liquid sheet instability in coflowing air stream. ICLASS-91, 15–18 July, Gaithersburg, MD, USA, pp. 679–686.

Eroglu, H., Chigier, N., Faragó, Z., 1991. Coaxial atomizer liquid intact lengths. Phys. Fluids A 3, 303–308.

Faragó, Z., Chigier, N., 1992. Morphological classification of disintegration of round liquid jets in a coaxial air stream. Atomizat. Sprays 2, 137–153.

Fernandes, E.C., Heitor, M.V., 1997. Simultaneous measurements of velocity, pressure, temperature and heat release in an oscillating flame. 90th Symposium of Propulsion and Energetics on the Advanced Non Intrusive Instrumentation for Propulsion Engines. AGARD 20–24 October, Bruxelles, Belgium.

Fraser, R.P., Dombrowski, N., Routley, J.H., 1963. The atomization of a liquid sheet by an impinging air stream. Chem. Eng. Sci. 18, 339–353.

Hagerty, W.W., Shea, J.F., 1955. A study of stability of plane fluid sheets. J. Appl. Mech. 22, 509–514.

Hardalupas, Y., Tsai, R.F., Whitelaw, J.H., 1998. Primary breakup of coaxial airblast atomisers. ILASS-Europe'98, 6–8 July, Manchester, England, pp. 42–47.

Karl, J., Huilier, D., Burnage, H., 1996. Mean behavior of a coaxial airblast atomized spray in a co-flowing air stream. Atomizat. Sprays 6, 409–433.

Lee, S.Y., 1985. Effect of condensation on the breakup of liquid sheet-experimental observations. ICLASS-85, Paper VIB/2, 9–10 July, London, UK.

Lefebvre, A.H., 1992. Energy considerations in twin-fluid atomization. Trans. ASME, J. Eng. Gas Turbines Power 114, 89–96.

Lee, C.P., Wang, T.G., 1986. A theoretical model for the annular jet instabillity. Phys. Fluids A 29, 2076–2085.

Lozano, A., Call, C.J., Dopazo, C., Garcia-Olivares, A., 1996. Experimental study of the atomization of a planar liquid sheet. Atomizat. Sprays 6, 77–94.

Mansour, A., Chigier, N., 1990. Disintegration of liquid sheets. Phys. Fluids A 3, 2971–2980.

Mansour, A., Chigier, N., 1991. Dynamic behavior of liquid sheets. Phys. Fluids A 2, 706–719.

Rizk, N.K., Lefebvre, A.H., 1980. The influence of liquid film thickness on airblast atomization. Trans. ASME, J. Eng. Power 102, 706–710.

Stapper, B.E., Sowa, W.A., Samuelsen, G.S., 1992. An experimental study of the effects of liquid properties on the breakup of a two-dimensional liquid sheet. Trans. ASME, Eng. Gas Turbine Power 114, 39–45.